Thomas Wittenberg*, Wolfgang Becker, Thomas Bocklitz, Lukas Braun, Ralf Hackner, Niels Lemke, Arkadiusz Miernik, Philippe-Fabian Pohlmann, Rodrigo Suarez-Ibarrola, Christoph Krafft

First results of computer-enhanced optical diagnosis of bladder cancer

Abstract Bladder cancer is the sixth leading cancer cause worldwide. Non-muscle invasive tumors can be diagnosed and treated endoscopically. Based on biopsies alone, pathologists cannot determine the spatial organization of specimens, their relationship with each other, or their complete removal. To extend *white light cystoscopy* as the gold standard for bladder cancer detection, diagnosis and removal of small or flat lesions, new image-based technologies have been investigated. These include a stereo-cystoscope for improved orientation and navigation, computation of 2D and 3D panoramic images for extended visualization and documentation, as well as label-free fiber-based fluorescence-lifetime imaging (FLIM) and Raman-spectroscopy in combination with statistical data analysis. Combining all these technologies, cystoscopy can will be further enhanced to include new diagnostic possibilities.

Keywords: Urology, 3D-Endoscopy, Panorama imaging, Raman spectroscopy, FLIM,

https://doi.org/10.1515/cdbme-2020-3062

1 Introduction

In the European Union (EU), bladder cancer (BCa) is the sixth leading cause of cancer accounting for 124,000 new cases annually and costing the EU health care systems 2.9€ billion in 2012 [1] In Germany, BC represented 4.7% of all new cancer cases and 3.2% of all cancer-related deaths in 2014 [2]. While muscle-invasive disease is treated with radical cystectomy, non-muscle invasive tumors are diagnosed and treated endoscopically. Nevertheless, based on cystoscopically obtained biopsies, a pathologist cannot accurately determine the spatial organization of specimens, their relationship with each other, or the complete removal of tumors from the bladder wall´s inner surface. In certain cases, such as in locally invasive and high-grade tumors, urologist have to perform a second transurethral resection at the same site to ensure a complete tumor resection. Currently, *white light cystoscopy* is the gold standard for BCa diagnosis. Using a rigid or flexible cystoscope, the bladder´s iner wall is systematically examined for suspicious findings or lesions. Many of these lesions, especially flat, small, or only slightly textured tissue changes are difficult to diagnose (see Fig. 1 left side). Thus, in order to reduce recurrence and progression rates, and support the urologist and pathologist with diagnostic and interventional procedures, various optical sensor systems have been introduced in the past. Among these are e.g. photodynamic diagnosis (PDD) [3], narrow band imaging (NBI) [4], confocal laser endoscopy (CLE) [5,6] or optical coherence tomography (OCT) [7,8].

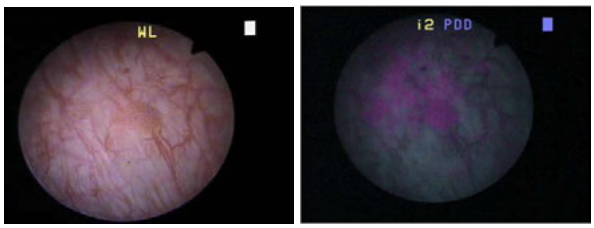

Figure 1: Example of a white-light cystoscopic image with a hard to detect flat lesions (left), and corresponding blue light image where the lesion is depicted with a color contrast.

In the case of PDD, (fluorescence or *blue light cystoscopy*) patients receive an intravesical instillation with *hexaminonlevulinate* to induce fluorescence in potentially malignant tissue, which can be depicted using blue light (see Fig. 1 right). Nevertheless, PDD is associated with considerable effort and resources (stress on the patient due to catheter insertion, time for instillation and distribution in the bladder, additional endoscopic equipment, cost of substance). Even though NBI does not relate to bladder installations, it is dependent on an additional light-source as well as the experience of the observer. Even though CLE and OCT are established technical methods, they

***Corresponding author: Thomas Wittenberg:** Fraunhofer IIS, Wolfsmantel 33, 91058 Erlangen, Germany, e-mail: wbg@fraunhofer.de, **R. Hackner:** Fraunhofer IIS, Erlangen; **T. Bocklitz, C. Krafft:** Leibniz-IPHT; **W. Becker, L. Braun:** Fa. Becker & Hickl, Berlin; **P. Pohlmann, A. Miernik, R. Suarez-Ibarrola:** Univ.-Klinik Freiburg; **MN. Lemke:** Fa. Schölly, Denzlingen

lack larger clinical studies. Ultimately, surgeons make a decision whether an area is malignant and on its resection based on individual assessment and personal experience.
Hence, new optical procedures are needed for improved diagnosis, for better differentiation between low- and high-grade tumors, as well as on non-muscle and muscle invasive disease.

2 Methods

To potentially support urologists during the assessment and diagnosis of small, flat or only slightly textured lesions in the urinary bladder, within the interdisciplinary research project 'UroMDD' (endoscopic panorama imaging and fiberoptic spectroscopy for multi-modal diagnostic in urology), various new aspects for image-based computer-assisted diagnosis have been investigated and developed, which shall be described in the next sections. Among these are a stereo-cystoscope for improved orientation and navigation (section 2.1), computation and interactive visualization of 2D and 3D panoramic bladder wall images for enhanced documentation and quality control (section 2.2), as well as label-free fiber-based diagnostic tissue sensing using fluorescence-lifetime imaging (FLIM) (section 2.3) and Raman-spectroscopy in combination with statistical data analysis (section 2.4). All acquired data can be fused and displayed within the bladder panoramas.

2.1 Stereo-Cystoscope

For an improved detection and treatment of lesions in the human bladder as well for better orientation and navigation, a digital stereo-cystoscope was designed and prototype built. This prototype has a diameter of 4 mm and incorporates two tiny digital sensors at the distal end. Fig. 2 depicts an example stereo view into a cadaver phantom (cow's knee) with visible depth structures.

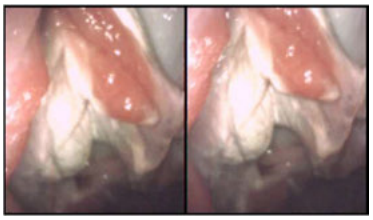

Figure 2: Example stereo data obtained in a cadaver phantom obtained with early prototype of the new digital stereo endoscope.

2.2 Panoramic imaging

Besides an improved urothelial carcinoma detection (see Sections 2.3+2.4), a comprehensive documentation of all findings is also essential. The current European Association of Urology guidelines strongly recommend the description of all macroscopic findings on a bladder diagram [10]. Nevertheless, this method lacks accuracy and findings are susceptible to inter and intra-observer variability. An alternative to this shortcoming are photo-documentation systems. Most cystoscopy systems provide the possibility for photo or video documentation. While images do not provide the context of a finding and may lead to misinterpretations, videos are more complex and require large volumes of data. To improve on this methodology, an image-based panoramic documentation system for cystoscopic examinations was developed, which yields high resolution images in real-time with direct visual feedback [11,12]. Using such image panoramas, see Fig. 3, lesions can be depicted in relation to anatomical land marks such as the ureteral orifices.

Figure 3: Example of a panoramic image of the bladder.

Similarly, panoramic images computations can be extended to stereoscopic endoscopic data [13]. In this case, additional to the texture mosaic (as in Fig. 3), the hollow´s geometry can be reconstructed, see Fig. 4.

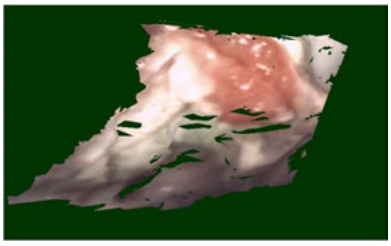

Figure 4: Image panorama with depth ("3D-panorma") based on stereo data (cf. Fig 1) obtained with a prototype of 4 mm stereo-cystoscope in a cadaver experiment.

2.3 FLIM

Fluorescence lifetime imaging (FLIM) is largely independent of variations in the chromophore concentration, irradiation intensity or processes such as photo-bleaching. Therefore, the quantification of fluorophores using FLIM is more reliable than using fluorescence intensity. FLIM has already provided molecular contrast in in-vivo bladder studies [14].
Within this study, a ps-diode laser at 375 nm excited freshly excised urothelial samples taken within 20 minutes after transurethral resection. The induced NAD(P)H autofluorescence is spectrally filtered at 447/60 and imaged by laser scanning.

Subsequently, the samples were fixed in formalin and analysed by an experienced pathologist. Fig. 5 shows excised tissue

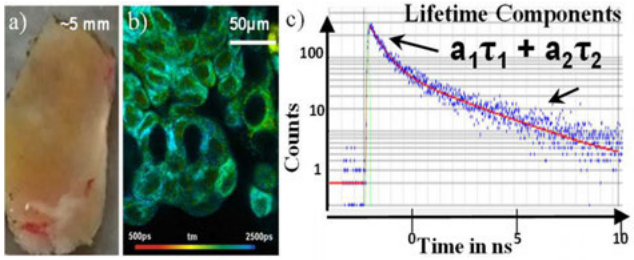

with tumor cells, a false color FLIM-image of the mean-lifetime and the double-exponential decay curve [15].

Figure 5: a) Tissue resected from human bladder. Lower white area shows tumor. b) NADH-FLIM image of from healthy cells. Color indicates tm. c) NADH fluorescence lifetime curve with components τ1 and τ2.

2.4 Raman Spectroscopy

Raman spectroscopy is based on inelastic scattering of monochromatic light. The spectrum of molecular vibrations enables highly specific identification of biomedical specimens [16]. Here, Raman images were registered at 785 nm excitation in a sequential acquisition mode at 250 µm step size. Control and tumor specimens were prepared from human bladder resections. Their sizes ranged from ca. 5-10 mm. Samples were placed in a sample chamber and covered with a calcium fluoride window to protect the samples from drying. Photographs are shown in Fig. 6. The liquid around the samples is optimal cutting temperature medium in which the specimens were immersed before storage in the tissue bank. Control tissue appears red whereas tumor tissue has a brighter hue. Of particular interest is tumor 2 because the bright region in the center is surrounded by a red region.

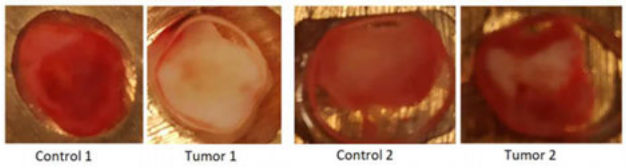

Figure 6: Tissue samples from human bladder resections. Control and control tissue were prepared from patient 1 and 2.

3 Results

The ***FLIM-images*** are fitted in each pixel with a double-exponential decay model. The amplitude weight of the fast component a1 is shown in Fig. 7. a1-FLIM-images show three samples classified by a pathologist according to the WHO 2016 classification for urothelial carcinoma: healthy, healthy/ inflammation, high-grade tumor. There is a well-defined difference in a1 between healthy and tumor cells. We find that healthy cells show a1~0,66 while cancer cells show a1 ~ 0,76. The increase of the a1 values indicates the change of metabolism in tumor cells [17]. All 15 investigated samples confirm direct correlation of the a1 value with the pathological result with a boarder value of a1 ~ 0,71 (red line in Fig. 7).

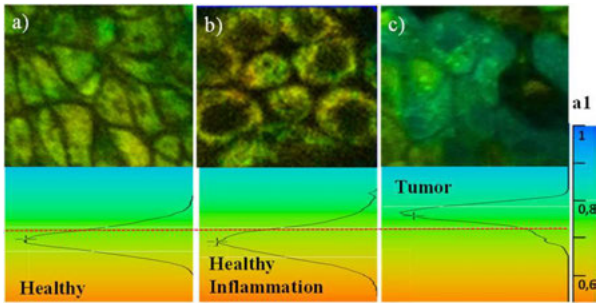

Figure 7: a) NAD(P)H a1- FLIM images of human bladder. Images indicate metabolism in a) normal tissue, b) inflammation and c) high-grade tumor. Changes in a1 agree with histological findings.

The results show that TCSPC fluorescent spectral analysis successfully distinguishes normal urothelial cells from urothelial carcinoma. The mean lifetime distribution, amplitude-weighted lifetime (tm), and amplitude distribution of the fast decay component (a1) in the NAD(P)H and FAD images varied between normal and tumor cells. Thus, FLIM investigations further endorse the concept that tumor tissue relies on a different metabolic equilibrium than normal tissue, in which endogenous fluorophores NAD(P)H and FAD are mainly involved.

The ***Raman data*** sets were decomposed into endmember loadings and scores by vertex component analysis without further pre-processing. The results represent the spectra and concentrations of the most dissimilar components. Examples are given in Fig. 8. The Raman spectra of control tissue are dominated by spectral contributions of proteins with α helical structure as evident from the bands at 934, 1270 and 1655 cm^{-1}. The other labeled bands are assigned to aromatic and aliphatic amino acid residues. The abundance images display that this component is most abundant in the right part of control sample #1 and in the central part of control sample #2. The Raman spectra of tumor tissue are also dominated by spectral contributions of proteins, however with different secondary structures as evident from more intense bands and band shifts at 922, 938, 1246 and 1665 cm^{-1}. These changes together with typical bands of proline and hydroxyproline at 815 and 855 cm^{-1} point to elevated content of fibrous proteins such as collagen [18]. The abundance plots show that tumor tissue is homogenously distributed in sample #1, only the upper portion is assigned to tumor in sample #2 which is consistent with the photograph in Fig. 6. Results are confirmed by histopathological inspection of parallel, hematoxylin and eosin stained tissue section that

will be presented in an accompanying paper together with the other components.

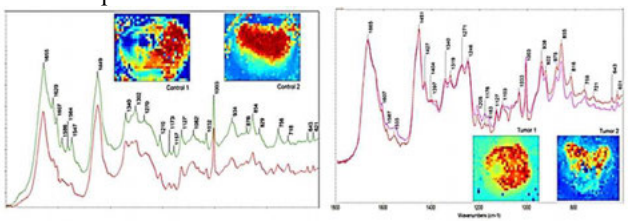

Figure 8: Vertex component analysis of Raman images of bladder tissues. Endmember spectra and abundance plots are shown for control (left) and tumor tissue (right)

Lastly, the ***simultaneous visualization*** of a bladder panorama *together* with images and data of suspicious findings, as e.g. from FLIM and Raman data of tumorous lesions (depicted in Fig. 9), can strongly enhance an examination´s completeness as well as lesion documentation, since these can now be related to their correct anatomical context.

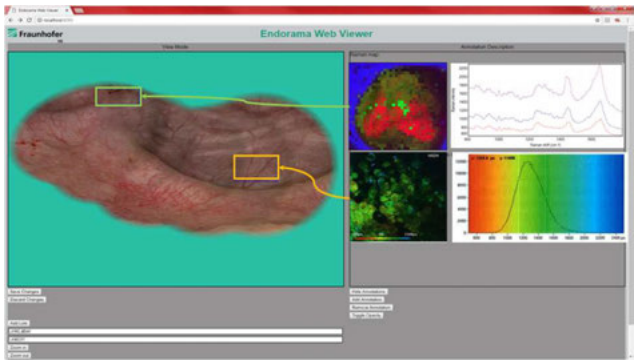

Figure 9: Simultaneous visualization of a panoramic bladder image together with results from Raman spectroscopy (top right) and FLIM data (center right). It can be seen that additional results can now be placed into the correct anatomical context, thus improving the documentation and location of suspicious finding.

4 Discussion and Conclusion

Our preliminary results are encouraging to develop new intra-operative tools outperforming the diagnostic accuracy of white light cystoscopy. A new endoscopic instrument integrating glass-fibers used to transmit spectral data to identify malignant lesions and determining their tumor grade in real-time during cystoscopic procedures would be an invaluable tool in the management of bladder cancer to decrease recurrences, improve patient outcomes and provide cost-effective treatment pathways. The employed FLIM and Raman technology have the potential to be incorporated into cystoscopes and ureteroscopes in a miniaturized manner for a thorough evaluation of the lower and upper urinary tract. Furthermore, panoramic documentation allowing the depiction of spatial relationships of detected lesions within the bladder as well as the integration of FLIM and Raman data for direct visual assessment will help to improve the documentation in cystoscopy.

This work has partially been funded by the German Federal Ministry of Education and Research (BMBF) under the project UroMDD (03ZZ0444).

References

[1] Ferlay et al.: Estimating the global cancer incidence and mortality in 2018. Int J Cancer 144, 1941-53, 2019

[2] Robert Koch Institute, Cancer in Germany 2013

[3] Jocham et al: Photodynamic diagnosis in urology: state-of-the-Art. Europ. Urology 53: 1138-50, 2008.

[4] Hsueh & Chiu: Narrow band imaging for bladder cancer AJUrol 3(3):126-9, 2016.

[5] Chen & Liao: Confocal laser endomicroscopy of bladder and upper tract urothelial carcinoma: A new era of optical diagnosis? Curr Urol Rep 15(9): 437, 2014.

[6] Liem et al.: Validation of confocal laser endomicroscopy features of bladder cancer: The next step towards real-time histologic grading. Eur. Urol. Focus 15;6(1):81-7, 2020.

[7] Freund et al.: Optical coherence tomography in urologic oncology: a comp. review. SN Compr. Clin Med.1: 67-84, 2019.

[8] Malmström et al: Non-muscle-invasive bladder cancer: a vision for the future. Scand. JUro 51(2) 87-94, 2017.

[10] Babjuk et al: EAU Guidelines on non-muscle-invasive urothelial carcinoma of the bladder: Europ Urol. 71: 447-46, 2017.

[11] Bergen: Real-time endoscopic image stitching for cystoscopy. PhD Thesis, Univ. Koblenz-Landau 2017.

[12] Hackner et al: Evaluation of different bladder phantoms for panoramic cystoscopy. Procs CURAC 2018: pp. 247-52.

[13] Wittenberg et al: Panorama-Endoscopy of the abdomen: from 2D to 3D. Proc's CURAC 2017: pp. 53-7.

[14] Cicchi et al: Time- & spectral-resolved 2-photon imaging of healthy bladder mucosa & carcinoma in situ. Opt. Express 18(4): 3840-9, 2010.

[15] Pastore et al: Non-invasive metabolic imaging of melanoma progression. Exp. Dermatol. 26, 607-14, 2017.

[16] Krafft et al: Label-free molecular imaging of biological cells and rissues by linear and nonlinear raman spectroscopic approaches. Angew. Chemie 56(16):4392-430, 2016.

[17] Becker at al: Metabolic imaging by simultaneous FLIM of NAD-(P)H and FAD, Proc. SPIE 10882, 2019.

[18] Krafft et al: Raman and FTIR microscopic imaging of colon tissue: a comparative study. J BioPhot. 1(2) 154-169, 2008.